

V2X-DGW: Domain Generalization for Multi-agent Perception under Adverse Weather Conditions

Baolu Li^{1*}, Jinlong Li^{1*}, Xinyu Liu¹, Runsheng Xu², Zhengzhong Tu³,
Jiacheng Guo¹, Xiaopeng Li⁴, and Hongkai Yu^{1†}

¹ Cleveland State University

² University of California, Los Angeles

³ University of Texas at Austin

⁴ University of Wisconsin-Madison

Abstract. Current LiDAR-based Vehicle-to-Everything (V2X) multi-agent perception systems have shown the significant success on 3D object detection. While these models perform well in the trained clean weather, they struggle in unseen adverse weather conditions with the real-world domain gap. In this paper, we propose a domain generalization approach, named *V2X-DGW*, for LiDAR-based 3D object detection on multi-agent perception system under adverse weather conditions. Not only in the clean weather does our research aim to ensure favorable multi-agent performance, but also in the unseen adverse weather conditions by learning only on the clean weather data. To advance research in this area, we have simulated the impact of three prevalent adverse weather conditions on two widely-used multi-agent datasets, resulting in the creation of two novel benchmark datasets: OPV2V-w and V2XSet-w. To this end, we first introduce the Adaptive Weather Augmentation (AWA) to mimic the unseen adverse weather conditions, and then propose two alignments for generalizable representation learning: Trust-region Weather-invariant Alignment (TWA) and Agent-aware Contrastive Alignment (ACA). Extensive experimental results demonstrate that our V2X-DGW achieved improvements in the unseen adverse weather conditions.

Keywords: 3D Object Detection, Vehicle-to-Everything (V2X), Multi-agent Perception, Domain Generalization, Adverse Weather

1 Introduction

The advent of multi-agent perception systems has marked a significant leap forward in surmounting the inherent limitations of single-agent perception from the challenges of perceiving range and occlusion [3, 45]. Leveraging Vehicle-to-Everything (V2X) communication technology for the exchange of LiDAR and camera data, these systems have demonstrated a substantial enhancement in

* Equal contribution. † Corresponding author: h.yu19@csuohio.edu

perception performance over their single-agent counterparts [39, 48]. Notably, the utilization of LiDAR sensors, preferred for their insensitivity to lighting conditions thereby facilitating effective operation both day and night, has become a cornerstone in the development of state-of-the-art cooperative perception methodologies [3, 20, 22, 39, 48]. However, these methods, predominantly reliant on supervised learning, presuppose a consistent distribution of features between training and testing datasets—a hypothesis that often fails under the real-world variability of adverse weather conditions, thus presenting a barrier to the safety-ensured autonomous driving.

Recent endeavors in Unsupervised Domain Adaptation (UDA) methods have sought to address this shortfall by feeding the unlabeled target-domain data in the model training, aiming to ameliorate performance degradation within specific target domains [15, 25, 38]. Despite their efficacy in these target domains, UDA methods might show limited generalizability to unseen data corrupted by adverse weather conditions, leading to a pronounced performance decline. This predicament stems from notable unknown domain gaps between the training data and unseen testing data. To solve this challenging problem, this paper is dedicated to exploring the potential of solely using labeled clean-weather LiDAR data for training, with a focus on enhancing the Domain Generalization (DG) capabilities of multi-agent perception systems in different unseen adverse weather conditions. We discover and summarize three specific factors for the domain gap between clean to adverse weather conditions of multi-agent perception, as detailed below.

- **Perception Range Reduction:** Snowflakes, raindrops, or fog particles might temporarily block the LiDAR’s line of sight, causing loss or erroneous data in the point cloud. This dynamic occlusion reduces the vehicle’s ability to perceive its surroundings accurately in the real world.
- **Point Cloud Degradation:** Severe weather conditions, such as fog and rain, might significantly change the characteristics compared to clean weather, such as optical attenuation in the atmosphere, surface reflectivity changes, dynamic occlusions. These factors reduce the amount of effective signal returned to the LiDAR, affecting the integrity and accuracy of the point cloud.
- **Accumulated Damages on Perception:** The adverse weather conditions impair each agent’s perception, so the multi-agent perception system might have accumulated damages due to the V2X information sharing.

Based on the previous related works [9, 10, 14, 40], there are reduced perception range and point cloud degradation in fog, rain, and snow scenarios, which might result in potential accumulated damages to the whole perception system. The domain gaps by the above three factors could result in significant performance decline in multi-agent perception under adverse weather conditions, which have never been well studied before. Due to the difficulties of collecting multi-agent data with communication and considering the adverse weather in the real world, to facilitate research in this area, we leverage the OPV2V [48] and V2XSet [47] datasets of multi-agent perception, by simulating the effects of

Multi-agent Perception

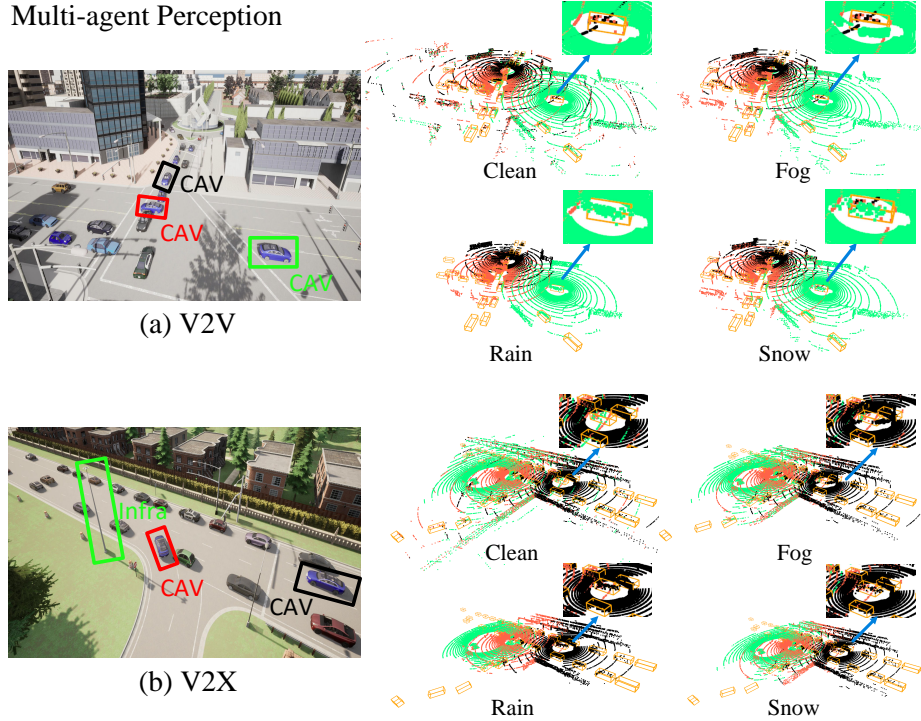


Fig. 1: Vehicle-to-Vehicle (V2V) and Vehicle-to-Everything (V2X) examples for multi-agent perception system under adverse weather. Reduced perception range can be found and the point cloud degradation is enlarged. Different-color agent in the left snapshot has the corresponding color in the right point clouds. CAV: Connected and Automated Vehicle, Infra: Infrastructure. Best view in color.

three common adverse weather conditions, *i.e.*, *Fog*, *Rain*, *Snow* to generate two new adverse weather datasets, namely OPV2V-w and V2XSet-w, to study this scientific problem as shown in Fig. 1.

This paper proposes a novel domain generalization approach called V2X-DGW for LiDAR-based 3D object detection of V2X multi-agent perception systems under adverse weather conditions. This approach is designed to improve performance in unseen adverse weather conditions, training exclusively on the clean-weather source data. First of all, we design a new Adaptive Weather Augmentation (AWA) to mimic the LiDAR point clouds in adverse weather conditions with reduced perception range and diverse degradation. We then propose two alignment techniques for the generalizable representation learning, namely Trust-region Weather-invariant Alignment (TWA) and Agent-aware Contrastive Alignment (ACA). Specifically, TWA is proposed for domain generalization in adverse weather conditions and ACA is used as a contrastive learning based regularization to shrink the accumulated damages on perception due to adverse weather. Finally, we conducted extensive experiments on our two new simulated adverse weather datasets, namely simulated OPV2V-w and V2XSet-w

from [47, 48], to justify the effectiveness of our proposed method. Our contributions are summarized as follows.

- To the best of our knowledge, we propose the **first research** of domain generalization for LiDAR-based V2X multi-agent perception systems under adverse weather conditions.
- To assess the impact of adverse weather on multi-agent perception systems, we simulate the effect of three common types of weather conditions: *Fog*, *Rain*, and *Snow*, on point cloud from the clean weather, utilizing the existing OPV2V and V2XSet datasets to create two novel adverse weather benchmark datasets, namely OPV2V-w and V2XSet-w.
- We propose a new Adaptive Weather Augmentation (AWA) to mimic the unseen adverse weather conditions from the clean-weather source data only and design two new alignment methods for the generalizable representation learning: Trust-region Weather-invariant Alignment (TWA) for domain generalization in unseen adverse weather conditions and Agent-aware Contrastive Alignment (ACA) as a contrastive learning based regularization to relieve the accumulated damages by adverse weather.

2 Related Work

Multi-agent Perception. Multi-agent perception systems transcend the constraints of single-vehicle systems by utilizing information via collaboration modules, enhancing effectiveness and results of multi-agent perception tasks [39, 43, 47, 48]. Generally, three methods are mainly used for combining observations from multiple vehicles: merging raw data [4, 35], integrating features during processing [3, 20, 22, 39, 48], and output fusion [1, 50]. Attfuse [48] utilizes self-attention models to enhance the sharing features for V2V perception system. SCOPE [49] presents a learning-based framework that targets multi-agent challenges, prioritizing the temporal context of the ego agent. CoBEVT [44] and V2X-ViT [47] introduces a unified Vision Transformer architecture to integrate features from multi-agent perception systems. While these methods demonstrate remarkable performance in multi-agent perception, they have primarily been evaluated under clear weather conditions, neglecting the impact of adverse weather. This paper aims to address these domain gaps by considering the effect of adverse weather conditions on multi-agent perception system.

Deployment of Multi-agent System. While multi-agent perception systems present numerous benefits, establishing a practical real-world multi-agent perception system encounters several obstacles. These challenges include susceptibility to adversarial attacks [20, 37], lossy communication [23, 51], localization inaccuracies [29, 47], communication delay [47], data discrepancy [21, 22], and model heterogeneity [42]. To prevent the erosion of collaborative advantages posed by these challenges, some strategies have been presented to bolster system robustness. S2R-ViT [22] is introduced to address the deployment gap and feature gap between simulation and reality in multi-agent cooperative perception tasks. FDA [21] is proposed to enable cross-domain learning in multi-agent

perception systems to reduce data silos caused by distribution gap in multi-agent perception. LCRN [23] mitigates the lossy communication challenge by tackling packet loss during communications. HEAL [28] is introduced as the first extensible heterogeneous collaborative perception framework, establishing a unified feature space and aligning new agents to it. However, adverse weather conditions such as rain, snow, and fog pose significant challenges for single-agent systems relying on camera or LiDAR sensory data [9, 10, 12, 14, 24, 33]. To mitigate this issue, various physics-based simulation methods [9, 14] have been introduced to generate point clouds across diverse weather scenarios. Nevertheless, the impact of adverse weather conditions on multi-agent perception systems has not been previously investigated. Thus, our aim is to enhance the domain generalization capability of multi-agent systems under adverse weather conditions.

Domain Generalization. Domain generalization (DG) is aimed at achieving the excellent performance in unseen domains by exclusively learning from source domains. Current DG methods have been extensively explored object detection [17, 38], semantic segmentation [15, 25, 36, 41] and reinforcement learning [11, 32] tasks in 2D and 3D computer vision tasks. As for strategies of DG employing multiple sources, which encompasses techniques such as the disentanglement of domain-specific and domain-invariant features [2, 27, 52], alignment of source domain distributions [5, 19, 31], and domain augmentation [54, 55]. For example, INB-Net [34] merges Instance Normalization (IN) with batch normalization to learn appearance invariant feature while maintaining content information. MLDG [18] is introduced as a meta-learning approach that synthesizes virtual testing domains during training to improve generalization to novel domains. These approaches have been instrumental in navigating the complexities associated with learning from diverse source domains. However, the extension of DG to the 3D point cloud domain, particularly concerning LiDAR point clouds, remains relatively untapped because of distinct type of gap stemming from 3D point clouds compared with 2D images. Some recent studies [15, 41, 53] have analyzed the sparsity of point clouds in addressing DG issues. In this paper, we focus on investigating the impact of LiDAR-based object detection on multi-agent perception systems in adverse weather conditions. To reach this goal, we propose a DG approach tailored for multi-agent perception systems operating under adverse weather conditions.

3 Methodology

3.1 Adverse-Weather Benchmark for Multi-agent Perception

Existing datasets on multi-agent perception are all collected under the assumption of clean weather. In this paper, we employ state-of-the-art physics-based simulation methods on the existing multi-agent perception datasets (OPV2V [48] and V2Xset [47]) to create two new benchmarks: OPV2V-w and V2Xset-w, to assess the impact of harsh weather on cooperative perception.

Physics-based Simulation.

We consider three different harsh weather conditions: *Fog*, *Rain*, *Snow*, as they are more common in the real world. Physics-based point cloud simulation methods have shown its success to approximate real weather conditions. Here, we adopt three state-of-the-art physics-based point cloud simulation methods [9, 10, 14] for simulating *Fog*⁵, *Rain*⁶ and *Snow*⁷ conditions respectively with the publicized source code. These simulation methods are based on the physical reflection and geometrical optical model in LiDAR sensors. The most recent study [6] have corroborated the consistency of perception performance in synthetic weather data by the physics-based simulation with that observed in real-world data under adverse weather scenarios.

OPV2V-w and V2XSet-w. OPV2V [48] and V2XSet [47] are two large scale open benchmark datasets for LiDAR based multi-agent perception. Since both of them are collected from the same game engine software Carla [7], leveraging these datasets to focus on the impact of weather variations later. Here we deploy physics-based simulation methods on the testing sets of OPV2V and V2XSet, then obtain OPV2V-w and V2XSet-w to evaluate domain generalization under adverse weather conditions.

3.2 Overview of Architecture

The proposed framework of V2X-DGW is depicted in Fig. 3. Given a spatial graph of CAVs within the communication range in clean weather source data, the point clouds of ego and CAVs are denoted $\mathbf{P}_{ego}^s \in \mathbb{R}^{4 \times m}$ and $\mathbf{P}_{cav}^s \in \mathbb{R}^{4 \times m}$, respectively. We firstly deploy Adaptive Weather Augmentation \mathbf{A}_w on the clean weather data and obtain the augmented data $\mathbf{P}_{ego}^a \in \mathbb{R}^{4 \times m}$ and $\mathbf{P}_{cav}^a \in \mathbb{R}^{4 \times m}$. Then all of them are projected into 2D pseudo-image shape $\mathbf{I} \in \mathbb{R}^{C \times H \times W}$ by leveraging the PointPillar [16]’s Pillar Feature Net (PFN), defined as \mathbf{M} . In our framework, each CAV shares the same Encoder for LiDAR feature extraction in all conditions. The ego vehicle acquires the visual features of neighboring CAVs through wireless communication. The intermediate features aggregated from N surrounding CAVs in source and augmented data are denoted as $\mathbf{F}_{cav}^s \in \mathbb{R}^{N \times H \times W \times C}$ and $\mathbf{F}_{cav}^a \in \mathbb{R}^{N \times H \times W \times C}$, respectively. The ego intermediate features are denoted as $\mathbf{F}_{ego}^s \in \mathbb{R}^{1 \times H \times W \times C}$ and $\mathbf{F}_{ego}^a \in \mathbb{R}^{1 \times H \times W \times C}$, respectively. The intermediate features are then fused by the same Feature Fusion Network (FFN). Finally, the fused feature maps are fed into the same prediction header for 3D bounding-box regression and classification. Here we formulate the whole framework $\mathbf{DGW}(\cdot)$ as

$$\mathbf{I}_{cav}^s, \mathbf{I}_{cav}^a, \mathbf{I}_{ego}^s, \mathbf{I}_{ego}^a = \mathbf{M}(\mathbf{P}_{cav}^s, \mathbf{A}_w(\mathbf{P}_{cav}^s), \mathbf{P}_{ego}^s, \mathbf{A}_w(\mathbf{P}_{ego}^s)), \quad (1)$$

$$\mathbf{F}_{cav}^s, \mathbf{F}_{cav}^a, \mathbf{F}_{ego}^s, \mathbf{F}_{ego}^a = \mathbf{E}(\mathbf{TWA}(\mathbf{I}_{cav}^s, \mathbf{I}_{cav}^a), \mathbf{TWA}(\mathbf{I}_{ego}^s, \mathbf{I}_{ego}^a)), \quad (2)$$

⁵ https://github.com/MartinHahner/LiDAR_fog_sim

⁶ <https://github.com/velatkilic/LISA>

⁷ https://github.com/SysCV/LiDAR_snow_sim

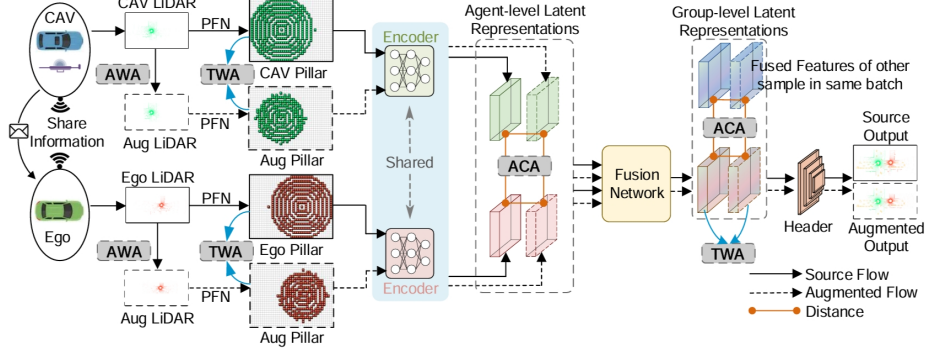


Fig. 2: Overview framework of the proposed V2X-DGW for domain generalization of multi-agent perception system in adverse weather. During the training stage, every agent has source flow (clean weather) and augmented flow (mimicked adverse weather). Pillar features are obtained from the Pillar Feature Net (PFN) [16], which is shown in bird view here.

$$\hat{\mathbf{F}}^s, \hat{\mathbf{F}}^a = \text{FFN}(\text{ACA}_a(\mathbf{F}_{cav}^s, \mathbf{F}_{cav}^a, \mathbf{F}_{ego}^s, \mathbf{F}_{ego}^a)), \quad (3)$$

$$\text{DGW}(\mathbf{P}_{cav}^s, \mathbf{P}_{ego}^s) = \mathbf{H}(\text{ACA}_g(\text{TWA}(\hat{\mathbf{F}}^s, \hat{\mathbf{F}}^a), *)), \quad (4)$$

where $\mathbf{E}(\cdot)$ is the Encoder for LiDAR feature extraction, $\text{FFN}(\cdot)$ is the Feature Fusion Network responsible for fusing the features of CAVs and the ego vehicle, $\hat{\mathbf{F}}$ is the fused feature extracted from $\text{FFN}(\cdot)$ and \mathbf{H} is the prediction header for 3D object detection, $\text{TWA}(\cdot)$ is the proposed Trust-region Weather-invariant Alignment (TWA), $\text{ACA}_a(\cdot)$ is the proposed Agent-aware Contrastive Alignment (ACA) in the agent-level, $\text{ACA}_g(\cdot)$ is the proposed Agent-aware Contrastive Alignment (ACA) in the group-level, and $*$ indicates the fused features of other samples in the same batch during training.

3.3 Adaptive Weather Augmentation

Based on our above discovery, the adverse weather conditions have 1) perception range reduction and 2) point cloud degradation in the LiDAR based point cloud data. Therefore, we design Adaptive Weather Augmentation (AWA) from two perspectives.

Mimic of Perception Range Reduction. Given $\mathbf{P}^s \in \mathbb{R}^{4 \times m}$ that contains a set of 3D points $\{P_i = (x_i, y_i, z_i) | i = 1, 2, 3, \dots, m\}$. The reception of LiDAR signals is subject to certain range limitations, thereby imposing maximal values on the x, y, and z coordinates of the point cloud data, denoted as x_m, y_m, z_m , respectively. Then, we sample the point clouds to reduce perception range by

$$\begin{aligned} \mathbf{P}^r &= \mathbf{S}_{x,y,z}(\mathbf{P}^s) \\ \text{s.t. } & |x_i/x_m| \leq \delta_x, |y_i/y_m| \leq \delta_y, |z_i/z_m| \leq \delta_z, \end{aligned} \quad (5)$$

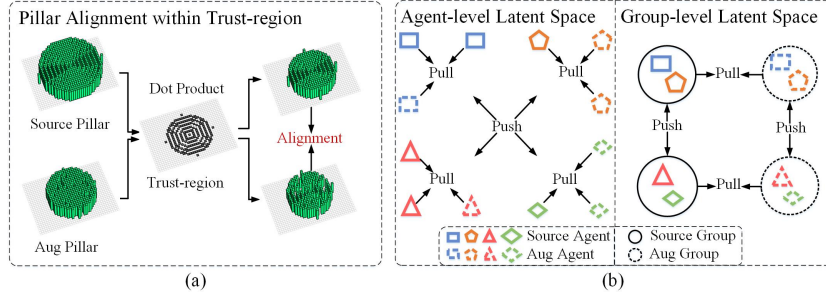


Fig. 3: Illustration of TWA and ACA. (a) Pillar-based weather-invariant alignment within Trust-region, (b) Agent-aware contrastive alignment in agent-level and group-level. Best view in color.

where $\mathbf{S}_{x,y,z}(\cdot)$ is the sampling function, $\delta_x, \delta_y, \delta_z$ are the thresholds of LiDAR receiving range and $\delta_x, \delta_y, \delta_z \sim U(\phi_L, \phi_U)$. ϕ_L and ϕ_U are the lower bound and upper bound of random sampling, respectively.

Mimic of Point Cloud Degradation. After the reception range decrease, we deploy three random degradation functions: random dropout $\Gamma(\cdot)$, random jittering $\Delta(\cdot)$ and random noise perturbation $\Theta(\cdot)$. The final AWA output \mathbf{P}^a can be obtained as

$$\mathbf{P}^a = \Theta(\Delta(\Gamma(\mathbf{P}^r))). \quad (6)$$

The AWA process is dynamically executed in real-time for each training iteration. This procedure generates augmented point cloud data, which are exclusively utilized for the purpose of simulating the unseen adverse weather conditions, so as to improve the model generalization capability.

3.4 Trust-region Weather-invariant Alignment (TWA)

To improve the generalization of multi-agent perception systems in adverse weather, aligning augmented flow (mimicked adverse weather) features with source flow (clean weather) features is essential. However, the direct alignment on the whole features might risk model training. Thus, we propose a trust-region weather-invariant alignment to guide the model focus on the reduced perception range.

Trust-region Weight. Most of current multi-agent perception systems leverage PointPillar [16] to process point clouds into pseudo-image, which is also called pillar and named as $\mathbf{I} \in \mathbb{R}^{C \times H \times W}$ and fed into Convolutional Neural Networks based Encoder. To address variations in point clouds from augmented and source settings, we define a trust-region $\mathbf{T} \in \mathbb{R}^{H \times W}$ on the pillar for weather-invariant learning, which is a 2D matrix that determines whether a perceived location should be considered or not. The each element of \mathbf{T} could be calculated by

$$\mathbf{T}(h, w) = \begin{cases} 1 & \text{if } \exists c \in \{1, \dots, C\} : \mathbf{I}^s(c, h, w) \neq 0 \wedge \mathbf{I}^a(c, h, w) \neq 0 \\ 0 & \text{otherwise.} \end{cases} \quad (7)$$

Pillar Alignment within Trust-region. We align each agent’s pillar features between source and augmented data, ensuring the Encoder to extract deep features within the trust region as shown in Fig. 3(a):

$$\mathcal{L}_{PAT} = \sum_{h=1}^H \sum_{w=1}^W \mathbf{T}(h, w) \cdot \sum_{c=1}^C \|\mathbf{I}^s(c, h, w) - \mathbf{I}^a(c, h, w)\|_1. \quad (8)$$

Fused Feature Alignment. After Feature Fusion Network (FFN), we align the augmented fused features with source fused features. This constraint enhances system robustness by minimizing weather-related disparities, defined as

$$\mathcal{L}_{FFA} = \sum_{h=1}^H \sum_{w=1}^W \sum_{c=1}^C \|\hat{\mathbf{F}}^s(c, h, w) - \hat{\mathbf{F}}^a(c, h, w)\|_1. \quad (9)$$

The total loss of TWA is formulated as $\mathcal{L}_{TWA} = \alpha_1 \mathcal{L}_{PAT} + \alpha_2 \mathcal{L}_{FFA}$, where α_1 and α_2 are balance coefficients.

3.5 Agent-aware Contrastive Alignment (ACA)

We propose Agent-aware Contrastive Alignment (ACA), as contrastive learning [13] based regularization, to relieve accumulated damages in multi-agent system during the adverse weather conditions.

ACA in Agent-level. Within a given scene, each agent/CAV is unique with a distinct ID. As shown in Fig. 3(b), we pull the feature distance of the same agent ID of the source and augmented data in the latent space, and we push the feature distance of the different agent IDs of the source and augmented data in the latent space. The contrastive loss of ACA in agent-level is formulated as

$$\mathcal{L}_{ACA_a} = -\frac{1}{B_a} \sum_{i=1}^{B_a} \sum_{p \in P(i)} \log \frac{\exp(\mathbf{F}_i^s \cdot \mathbf{F}_p^s / \tau) + \exp(\mathbf{F}_i^s \cdot \mathbf{F}_p^a / \tau) + \exp(\mathbf{F}_i^a \cdot \mathbf{F}_p^a / \tau)}{\sum_{j=1}^{B_a} \exp(\mathbf{F}_i^s \cdot \mathbf{F}_j^s / \tau) + \sum_{k=1}^{B_a} \exp(\mathbf{F}_i^a \cdot \mathbf{F}_k^a / \tau)}, \quad (10)$$

where B_a is the agent-level batch size in the training, $P(i)$ is the set of positive samples (the same-ID agent), τ is the temperature hyperparameter.

ACA in Group-level. After the FFN based fusion, the fused feature of multiple agents, $\hat{\mathbf{F}}^s$ or $\hat{\mathbf{F}}^a$, can be understood as group-level unit. As shown in Fig. 3(b), we pull the feature distance of the same group between the source and augmented data in the latent space, and we push the feature distance of the different groups within the source or augmented data in the latent space. The contrastive loss of ACA in group-level is formulated as

$$\mathcal{L}_{ACA_g} = -\frac{1}{B_g} \sum_{i=1}^{B_g} \log \frac{\exp(\hat{\mathbf{F}}_i^s \cdot \hat{\mathbf{F}}_i^a / \tau)}{\sum_{j=1}^{B_g} \exp(\hat{\mathbf{F}}_i^s \cdot \hat{\mathbf{F}}_j^s / \tau) + \sum_{k=1}^{B_g} \exp(\hat{\mathbf{F}}_i^a \cdot \hat{\mathbf{F}}_k^a / \tau)}, \quad (11)$$

where B_g is group-level batch size in training. The ACA loss function can be formulated as $\mathcal{L}_{ACA} = \beta_1 \mathcal{L}_{ACA_a} + \beta_2 \mathcal{L}_{ACA_g}$, where β_1 and β_2 are balance weights.

3.6 Overall Loss Function

Following [22], we use the focal loss [26] and smooth L_1 loss as the detection loss. Our final loss is the combination of detection loss and alignment losses as $\mathcal{L}_{total} = \mathcal{L}_{det}^s + \mathcal{L}_{det}^a + \mathcal{L}_{TWA} + \mathcal{L}_{ACA}$.

4 Experiments

4.1 Experiment Setup

Dataset. We utilize two popular multi-agent perception datasets for the domain generalization task for point cloud-based 3D object detection. OPV2V [48] is a comprehensive simulated dataset designed for V2V cooperative perception tasks, collected through the integration of the CARLA [7] and OpenCDA [46] platforms. It encompasses 73 varied scenes with CAVs. The dataset includes 6,764 frames for training and 2,719 frames for testing. V2XSet [47] is an expansive simulated dataset for V2X cooperative perception task, is also assembled utilizing CARLA. It features LiDAR data from a variety of autonomous vehicles and roadside infrastructures, synchronized within identical scenarios. The dataset is organized into training and testing subsets, containing 6,694 and 2,833 frames respectively. Here, we simulate adverse weather conditions only on the *testing sets* of these two datasets to generate OPV2V-w and V2XSet-w datasets for our experiments, as detailed in Section 3.1.

Evaluation Metrics. The final 3D vehicle detection accuracy are selected as our performance evaluation. Following [47, 48], we set the evaluation range as $x \in [-140, 140]$ meters, $y \in [-40, 40]$ meters, where all CAVs are included in this spatial range of the experiment. We measure the accuracy with Average Precisions (AP) at Intersection-over-Union (IoU) threshold of 0.5 and 0.7.

Compared Methods. To analyze the effect of adverse weather conditions on the perception performance of multi-agent system, two Domain Generalization (DG) methods, *i.e.*, IBN-Net [34], and MLDG [18], and three Domain Adaptation (DA) methods, *i.e.*, GRL [8], AdvGRL [24], and S2R-AFA [22] are implemented to be evaluated.

For the MLDG [18] setting, we employ two different strategies: randomly splitting each batch into meta-train and meta-test sets, denoted as $MLDG_a$, and splitting data by maximizing feature distances, denoted as $MLDG_b$. As for the domain adaptation methods, we follow the settings in [22].

Experimental Settings. This paper aims to enhance the perception performance of multi-agent systems via domain generalization technology under unseen adverse weather scenarios. We evaluate the detection performance across four weather conditions: clean, fog, rain and snow. All methods in the experiments employ the same cooperative perception method AttFuse [48] (as FFN), with the PointPillar based Encoder for fair comparison. We denote the AttFuse method without DA or DG as our Baseline, which is only trained on source data (clean weather) without AWA. For implementation of our V2X-DGW method, ϕ_L and ϕ_U are set to 0.5 and 0.8, α_1 and α_2 are set to 0.1 and 1, β_1 and β_2

are set to 0.01 and 0.01, τ is set to 0.07. We assess all methods under two key settings: 1) **OPV2V2ALL**. All DG methods including ours are trained on the OPV2V training set only. For DA methods, the labeled OPV2V training set serves as the source domain, while the unlabeled OPV2V training set added fog by Physics-based Simulation is utilized as the target domain during training. 2) **V2XSet2ALL**. In this setting, all DG methods including ours are trained on the V2XSet training set only. For DA methods, the labeled V2XSet training set is as the source domain, and the unlabeled V2XSet training set added fog by Physics-based Simulation is as the target domain during the training. For the above both settings, these methods are all tested/evaluated on the OPV2V-w and V2XSet-w with fog, rain, snow weather conditions.

Table 1: 3D detection performance on OPV2V2ALL setting. We show Average Precision (AP) at IoU=0.5, 0.7 on four weather conditions, respectively.

Method	OPV2V			OPV2V-w						V2XSet-w					
	clean			fog		rain		snow		fog		rain		snow	
	AP@0.5	AP@0.7		AP@0.5	AP@0.7	AP@0.5	AP@0.7	AP@0.5	AP@0.7	AP@0.5	AP@0.7	AP@0.5	AP@0.7	AP@0.5	AP@0.7
Baseline	88.10	79.48		67.55	59.40	71.17	58.34	60.51	46.96	63.04	55.92	65.05	53.64	63.86	52.47
IBN-Net [34]	85.08	77.07		66.45	58.31	68.92	59.55	55.28	45.80	61.20	52.92	62.27	53.54	61.03	51.94
MLGD _a [18]	87.68	78.13		67.23	59.30	68.55	57.50	58.86	47.67	63.12	55.07	63.15	53.38	62.06	52.29
MLGD _b [18]	83.93	73.49		62.73	54.52	63.94	54.39	51.52	42.78	58.36	51.01	57.17	48.88	55.88	47.55
Ours	89.23	81.52		71.35	64.35	75.31	67.98	65.80	58.38	66.66	60.37	70.61	63.77	69.44	62.68
GRL [8]	87.47	79.23		66.40	59.07	70.38	58.24	57.32	48.32	61.81	55.21	64.30	53.90	63.00	53.19
AdvGRL [24]	88.20	80.62		68.11	60.87	71.76	62.92	60.76	51.72	64.14	57.80	67.33	59.42	66.12	57.74
S2R-AFA [22]	87.34	78.65		67.53	59.30	70.64	57.62	60.43	46.68	63.04	55.75	64.75	53.06	63.54	51.90

4.2 Quantitative Evaluation

Performance in OPV2V2ALL. Table 1 shows the performance comparison on OPV2V2ALL setting, where all methods are evaluated on OPV2V, OPV2V-w and V2XSet-w testing sets, respectively. Without the effect of the adverse weathers, the Baseline without any DA or GD methods can gain a outstanding performance on OPV2V clean testing set. However when it is deployed on OPV2V-W testing sets, it drops 27.59% / 32.52% for AP@0.5/0.7 on the snow weather of OPV2V-W. It indicates that the cooperative perception system has significantly detrimental effects on performance under adverse weather conditions, which also underscores the importance of generalization capabilities. After applying the DA and GA methods, only a few have shown improved performance on the unseen weather domains. This could be attributed to the differences in domain gaps between 2D images and point clouds, as well as the ambiguity of appearance features in the LiDAR domain. Consequently, the performance enhancement achieved through learning appearance-invariant features may not be sufficient. While our method consistently outperforms comparative benchmarks in both clean and adverse weather conditions, as evidenced by the results presented in Table 1. For examples, our proposed method is improved by 5.29%/11.42% for for AP@0.5/0.7 on the snow weather of OPV2V-w. It un-

derscores the generalization capabilities of our proposed method for cooperative perception across a variety of adverse weather conditions.

Table 2: 3D detection performance comparison with V2XSet2ALL setting. We show Average Precision (AP) at IoU=0.5, 0.7 on clean, fog, rain, snow weather conditions, respectively.

Method	V2XSet		OPV2V-w						V2XSet-w					
	clean		fog		rain		snow		fog		rain		snow	
	AP@0.5	AP@0.7	AP@0.5	AP@0.7	AP@0.5	AP@0.7	AP@0.5	AP@0.7	AP@0.5	AP@0.7	AP@0.5	AP@0.7	AP@0.5	AP@0.7
Baseline	81.62	70.68	67.16	58.98	70.97	59.85	59.53	47.70	64.16	57.09	66.11	56.60	67.27	57.61
IBN-Net [34]	81.64	71.13	65.29	57.46	67.29	56.93	54.52	43.73	60.53	52.83	61.64	52.15	63.77	54.25
MLGD _i [18]	83.16	71.73	66.71	57.07	64.29	50.14	52.87	37.66	63.56	55.08	60.87	48.27	63.15	53.38
MLGD _i [18]	78.48	67.72	63.34	56.23	64.45	54.58	49.44	40.75	59.18	53.28	57.30	49.49	58.93	51.02
Ours	84.14	74.53	67.53	59.56	72.63	62.75	61.78	50.57	65.17	57.99	69.94	61.02	68.61	59.53
GRL [8]	82.67	72.80	67.17	58.87	69.95	59.11	58.76	47.88	62.90	56.18	64.45	55.48	66.38	56.76
AdvGRL [24]	82.64	72.09	67.26	58.49	67.50	56.35	59.46	48.59	63.87	55.63	63.35	52.81	64.43	53.82
S2R-AFA [22]	80.71	70.32	66.95	58.91	69.52	56.67	59.08	45.31	62.73	55.51	63.14	51.44	64.50	52.77

Performance in V2Vset2ALL. The LiDAR-based 3D object detection results on the **V2VSet2ALL** setting are presented in Table 2. Among all DA and GA methods, our proposed GA method achieves the best performance by eliminating the domain gap generated by the adverse weather conditions in the OPV2V-w and V2XSet-w testing sets. The outcomes under adverse weather conditions are akin to those observed when trained on the **OPV2V2ALL** setting. This similarity is attributable to both V2XSet and OPV2V being collected within the CARLA simulator [7], thereby mitigating extraneous influences and focusing on the impact of weather variations on multi-agent perception systems. Our method also achieve the best performance under adverse weather conditions.

Sensitivity to agent numbers. In a multi-agent perception system under adverse weather, the ego agent might be particularly vulnerable to the accumulated damages from other agents. Fig. 4 illustrates the impact of cooperative perception performance with varying numbers of agents under adverse weather. Intuitively, the cooperative perception performance should be improved with an increasing number of nearby agents/CAVs [48]. However, most comparison methods such as Baseline, GRL, AdvGRL, S2R-AFA, IBN-Net sometimes have decreasing cooperative detection performance with increasing agent numbers under some adverse weather scenarios. MLDG’s performance is sometimes keeping almost unchanged with the increasing agent numbers. This unreasonable phenomena might be due to their sensitivity to the accumulated damages from more agents in adverse weather. Differently, our V2X-DGW has continually improved cooperative detection performance with increasing agent numbers.

Accumulated damages in V2X. As depicted in (a) and (b) of Fig. 5, a single CAV can detect the highlighted vehicle under rainy weather conditions, whereas a multi-agent perception system with two CAVs even miss that vehicle within their perception range by the Baseline method. This type of accumulated damages caused by adverse weather can impair cooperative perception performance

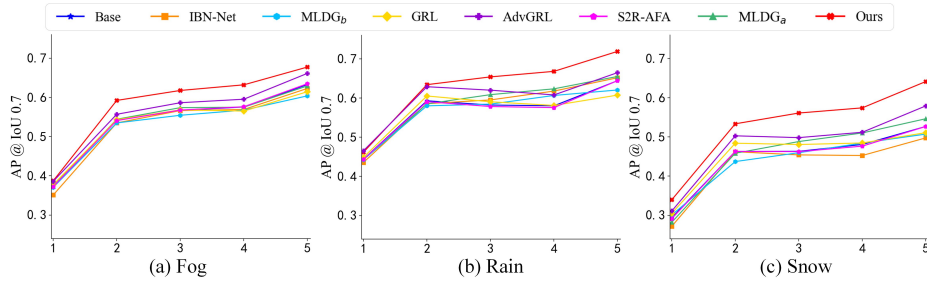


Fig. 4: Sensitivity to agent numbers. Detection (AP) with different agent/CAV numbers on OPV2V-w under adverse weather conditions.

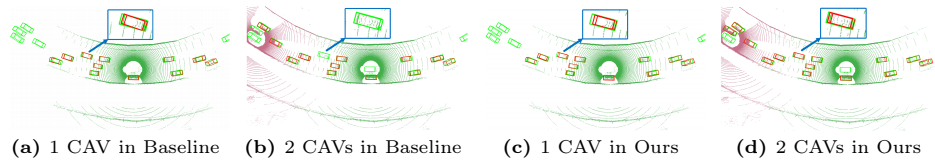


Fig. 5: Illustration of accumulated damages in the multi-agent system under adverse weather. One frame from V2XSet-w rain is shown as example here. Green and red 3D bounding boxes represent the ground truth and prediction respectively.

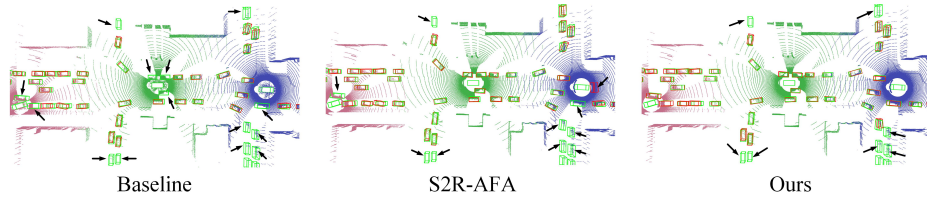


Fig. 6: 3D object detection visualization example under adverse weather. Green and red 3D bounding boxes represent the ground truth and prediction respectively. The detection errors are highlighted using black arrows. OPV2V-w fog weather is used as example here.

in real-world scenarios. However, our proposed V2X-DGW method demonstrates enhanced robustness against such cumulative damages under adverse weather.

3D detection visualization. Figure 6 presents the 3D detection visualization on OPV2V-w fog subset of the Baseline, S2R-AFA [22], and our proposed method. In clean weather, nearly all methods generate bounding boxes with high accuracy, closely aligning with the ground truths. However, when it is generalized to adverse weather conditions, both the baseline and DA methods exhibit detection errors. More critically, our method succeeds in identifying a greater number of dynamic objects, as evidenced by a higher match rate with ground-truth. This underscores the superior generalization capabilities of our proposed method.

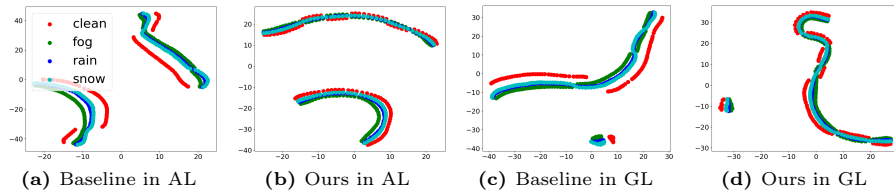


Fig. 7: Representation visualization with T-SNE [30]. We show two-type features in multi-agent system: Agent-Level (AL) and Group-Level (GL). Every point represents a data sample, and different color represents its different weather condition.

Representation visualization. We visualize the agent-level and group-level representation in V2X perception system using T-SNE [30]. As shown in Fig. 7, samples within the representation space resemble curves, attributable to the OPV2V-w consisting of continuous temporal frames. At both the agent-level and group-level, our proposed V2X-DGW method demonstrates a more cohesive clustering of samples across the four different weather conditions, as indicated by the tighter grouping of differently colored curves. This phenomenon is because of the implementation by our two alignments TWA and ACA. In other words, the generalizable weather-invariant features are learned by our V2X-DGW.

Ablation studies. To validate the effectiveness of our proposed components, we provide the quantitative comparison on detection result under clean, fog, rain, snow weather conditions in Table 3. Each component contributes to the model’s performance enhancement across all four weather conditions, validating the rationale behind the design of AWA, TWA, and ACA.

Table 3: Ablation study. Effects of the AWA, TWA, ACA components. The first row is the result by Baseline.

AWA	TWA	ACA	clean		fog		rain		snow	
			AP@0.5	AP@0.7	AP@0.5	AP@0.7	AP@0.5	AP@0.7	AP@0.5	AP@0.7
			88.10	79.48	67.54	59.39	71.17	58.33	60.51	46.96
✓			87.03	79.31	69.42	62.58	74.16	66.50	64.14	56.73
✓	✓		88.88	81.15	70.83	63.71	74.36	67.10	64.65	57.21
✓		✓	88.66	80.80	70.95	63.74	74.90	67.42	65.06	57.63
✓	✓	✓	89.23	81.15	71.35	64.34	75.30	67.97	65.80	58.38

5 Conclusion

In this paper, we propose a domain generalization approach for LiDAR-based 3D object detection on multi-agent perception system under adverse weather conditions. To investigate weather impact on multi-agent perception system, the effect of three common adverse weather conditions are simulated on the two publicized V2V/V2X datasets, and to obtain two adverse weather datasets: OPV2V-w and

V2XSet-w. To address the range reduction, point cloud degradation and accumulated damages in adverse weather, we first introduce the Adaptive Weather Augmentation (AWA) to simulate the unseen adverse weather domain, and then propose two alignments for generalizable representation learning: Trust-region Weather-invariant Alignment (TWA) and Agent-aware Contrastive Alignment (ACA). Extensive experiments show that our method achieved significantly improved performance in the unseen adverse weather conditions.

References

1. Arnold, E., Dianati, M., de Temple, R., Fallah, S.: Cooperative perception for 3d object detection in driving scenarios using infrastructure sensors. *IEEE Transactions on Intelligent Transportation Systems* **23**(3), 1852–1864 (2020) [4](#)
2. Bui, M.H., Tran, T., Tran, A., Phung, D.: Exploiting domain-specific features to enhance domain generalization. *Advances in Neural Information Processing Systems* **34**, 21189–21201 (2021) [5](#)
3. Chen, Q., Ma, X., Tang, S., Guo, J., Yang, Q., Fu, S.: F-cooper: Feature based cooperative perception for autonomous vehicle edge computing system using 3d point clouds. In: *ACM/IEEE Symposium on Edge Computing*. pp. 88–100 (2019) [1](#), [2](#), [4](#)
4. Chen, Q., Tang, S., Yang, Q., Fu, S.: Cooper: Cooperative perception for connected autonomous vehicles based on 3d point clouds. In: *IEEE International Conference on Distributed Computing Systems*. pp. 514–524. IEEE (2019) [4](#)
5. Chen, S., Wang, L., Hong, Z., Yang, X.: Domain generalization by joint-product distribution alignment. *Pattern Recognition* **134**, 109086 (2023) [5](#)
6. Dong, Y., Kang, C., Zhang, J., Zhu, Z., Wang, Y., Yang, X., Su, H., Wei, X., Zhu, J.: Benchmarking robustness of 3d object detection to common corruptions in autonomous driving. *IEEE Conference on Computer Vision and Pattern Recognition* (2023) [6](#)
7. Dosovitskiy, A., Ros, G., Codevilla, F., Lopez, A., Koltun, V.: Carla: An open urban driving simulator. In: *Annual Conference on Robot Learning*. pp. 1–16 (2017) [6](#), [10](#), [12](#)
8. Ganin, Y., Lempitsky, V.: Unsupervised domain adaptation by backpropagation. In: *International Conference on Machine Learning*. pp. 1180–1189. PMLR (2015) [10](#), [11](#), [12](#)
9. Hahner, M., Sakaridis, C., Bijelic, M., Heide, F., Yu, F., Dai, D., Van Gool, L.: Lidar snowfall simulation for robust 3d object detection. In: *IEEE/CVF Conference on Computer Vision and Pattern Recognition*. pp. 16364–16374 (2022) [2](#), [5](#), [6](#)
10. Hahner, M., Sakaridis, C., Dai, D., Van Gool, L.: Fog simulation on real lidar point clouds for 3d object detection in adverse weather. In: *IEEE/CVF International Conference on Computer Vision*. pp. 15283–15292 (2021) [2](#), [5](#), [6](#)
11. Hansen, N., Wang, X.: Generalization in reinforcement learning by soft data augmentation. In: *2021 IEEE International Conference on Robotics and Automation*. pp. 13611–13617. IEEE (2021) [5](#)
12. Heinzler, R., Schindler, P., Seekircher, J., Ritter, W., Stork, W.: Weather influence and classification with automotive lidar sensors. In: *IEEE Intelligent Vehicles Symposium*. pp. 1527–1534. IEEE (2019) [5](#)

13. Khosla, P., Teterwak, P., Wang, C., Sarna, A., Tian, Y., Isola, P., Maschinot, A., Liu, C., Krishnan, D.: Supervised contrastive learning. *Advances in neural information processing systems* **33**, 18661–18673 (2020) [9](#)
14. Kilic, V., Hegde, D., Sindagi, V., Cooper, A.B., Foster, M.A., Patel, V.M.: Lidar light scattering augmentation (lisa): Physics-based simulation of adverse weather conditions for 3d object detection. *arXiv preprint arXiv:2107.07004* (2021) [2](#), [5](#), [6](#)
15. Kim, H., Kang, Y., Oh, C., Yoon, K.J.: Single domain generalization for lidar semantic segmentation. In: *IEEE/CVF Conference on Computer Vision and Pattern Recognition*. pp. 17587–17598 (2023) [2](#), [5](#)
16. Lang, A.H., Vora, S., Caesar, H., Zhou, L., Yang, J., Beijbom, O.: Pointpillars: Fast encoders for object detection from point clouds. In: *IEEE Conference on Computer Vision and Pattern Recognition*. pp. 12697–12705 (2019) [6](#), [7](#), [8](#)
17. Lehner, A., Gasperini, S., Marcos-Ramiro, A., Schmidt, M., Mahani, M.A.N., Navab, N., Busam, B., Tombari, F.: 3d-vfield: Adversarial augmentation of point clouds for domain generalization in 3d object detection. In: *IEEE/CVF Conference on Computer Vision and Pattern Recognition*. pp. 17295–17304 (2022) [5](#)
18. Li, D., Yang, Y., Song, Y.Z., Hospedales, T.: Learning to generalize: Meta-learning for domain generalization. In: *AAAI Conference on Artificial Intelligence*. vol. 32 (2018) [5](#), [10](#), [11](#), [12](#)
19. Li, H., Pan, S.J., Wang, S., Kot, A.C.: Domain generalization with adversarial feature learning. In: *IEEE Conference on Computer Vision and Pattern Recognition*. pp. 5400–5409 (2018) [5](#)
20. Li, J., Li, B., Liu, X., Fang, J., Juefei-xu, F., Guo, Q., Yu, H.: Advgps: Adversarial gps for multi-agent perception attack. *IEEE International Conference on Robotics and Automation* (2024) [2](#), [4](#)
21. Li, J., Li, B., Liu, X., Xu, R., Ma, J., Yu, H.: Breaking data silos: Cross-domain learning for multi-agent perception from independent private sources. *IEEE International Conference on Robotics and Automation* (2024) [4](#)
22. Li, J., Xu, R., Liu, X., Li, B., Zou, Q., Ma, J., Yu, H.: S2r-vit for multi-agent cooperative perception: Bridging the gap from simulation to reality. *IEEE International Conference on Robotics and Automation* (2024) [2](#), [4](#), [10](#), [11](#), [12](#), [13](#)
23. Li, J., Xu, R., Liu, X., Ma, J., Chi, Z., Ma, J., Yu, H.: Learning for vehicle-to-vehicle cooperative perception under lossy communication. *IEEE Transactions on Intelligent Vehicles* (2023) [4](#), [5](#)
24. Li, J., Xu, R., Ma, J., Zou, Q., Ma, J., Yu, H.: Domain adaptive object detection for autonomous driving under foggy weather. In: *IEEE Winter Conference on Applications of Computer Vision*. pp. 612–622 (2023) [5](#), [10](#), [11](#), [12](#)
25. Li, M., Zhang, Y., Ma, X., Qu, Y., Fu, Y.: Bev-dg: Cross-modal learning under bird’s-eye view for domain generalization of 3d semantic segmentation. In: *IEEE/CVF International Conference on Computer Vision*. pp. 11632–11642 (2023) [2](#), [5](#)
26. Lin, T.Y., Goyal, P., Girshick, R., He, K., Dollár, P.: Focal loss for dense object detection. In: *IEEE International Conference on Computer Vision*. pp. 2980–2988 (2017) [10](#)
27. Liu, Z., Chen, G., Li, Z., Qu, S., Knoll, A., Jiang, C.: D2ifn: Disentangled domain-invariant feature learning networks for domain generalization. *IEEE Transactions on Cognitive and Developmental Systems* (2023) [5](#)
28. Lu, Y., Hu, Y., Zhong, Y., Wang, D., Chen, S., Wang, Y.: An extensible framework for open heterogeneous collaborative perception. In: *The Twelfth International Conference on Learning Representations* (2024) [5](#)

29. Lu, Y., Li, Q., Liu, B., Dianati, M., Feng, C., Chen, S., Wang, Y.: Robust collaborative 3d object detection in presence of pose errors. In: IEEE International Conference on Robotics and Automation. pp. 4812–4818. IEEE (2023) [4](#)
30. Van der Maaten, L., Hinton, G.: Visualizing data using t-sne. *Journal of Machine Learning Research* **9**(11) (2008) [14](#)
31. Matsuura, T., Harada, T.: Domain generalization using a mixture of multiple latent domains. In: AAAI Conference on Artificial Intelligence. vol. 34, pp. 11749–11756 (2020) [5](#)
32. Mazouze, B., Kostrikov, I., Nachum, O., Tompson, J.J.: Improving zero-shot generalization in offline reinforcement learning using generalized similarity functions. *Advances in Neural Information Processing Systems* **35**, 25088–25101 (2022) [5](#)
33. Montalban, K., Reymann, C., Atchuthan, D., Dupouy, P.E., Riviere, N., Lacroix, S.: A quantitative analysis of point clouds from automotive lidars exposed to artificial rain and fog. *Atmosphere* **12**(6), 738 (2021) [5](#)
34. Pan, X., Luo, P., Shi, J., Tang, X.: Two at once: Enhancing learning and generalization capacities via ibn-net. In: European Conference on Computer Vision. pp. 464–479 (2018) [5](#), [10](#), [11](#), [12](#)
35. Qiu, H., Huang, P.H., Asavisanu, N., Liu, X., Psounis, K., Govindan, R.: Autocast: scalable infrastructure-less cooperative perception for distributed collaborative driving. In: International Conference on Mobile Systems, Applications and Services. pp. 128–141 (2022) [4](#)
36. Sanchez, J., Deschaud, J.E., Goulette, F.: Domain generalization of 3d semantic segmentation in autonomous driving. In: IEEE/CVF International Conference on Computer Vision. pp. 18077–18087 (2023) [5](#)
37. Tu, J., Wang, T., Wang, J., Manivasagam, S., Ren, M., Urtasun, R.: Adversarial attacks on multi-agent communication. In: IEEE/CVF International Conference on Computer Vision. pp. 7768–7777 (2021) [4](#)
38. Vedit, V., Engilberge, M., Salzmann, M.: Clip the gap: A single domain generalization approach for object detection. In: IEEE/CVF Conference on Computer Vision and Pattern Recognition. pp. 3219–3229 (2023) [2](#), [5](#)
39. Wang, T.H., Manivasagam, S., Liang, M., Yang, B., Zeng, W., Urtasun, R.: V2vnet: Vehicle-to-vehicle communication for joint perception and prediction. In: European Conference on Computer Vision. pp. 605–621. Springer (2020) [2](#), [4](#)
40. Wu, J., Xu, H., Zheng, J., Zhao, J.: Automatic vehicle detection with roadside lidar data under rainy and snowy conditions. *IEEE Intelligent Transportation Systems Magazine* **13**(1), 197–209 (2020) [2](#)
41. Xiao, A., Huang, J., Xuan, W., Ren, R., Liu, K., Guan, D., El Saddik, A., Lu, S., Xing, E.P.: 3d semantic segmentation in the wild: Learning generalized models for adverse-condition point clouds. In: IEEE/CVF Conference on Computer Vision and Pattern Recognition. pp. 9382–9392 (2023) [5](#)
42. Xu, R., Chen, W., Xiang, H., Xia, X., Liu, L., Ma, J.: Model-agnostic multi-agent perception framework. In: IEEE International Conference on Robotics and Automation. pp. 1471–1478. IEEE (2023) [4](#)
43. Xu, R., Li, J., Dong, X., Yu, H., Ma, J.: Bridging the domain gap for multi-agent perception. In: 2023 IEEE International Conference on Robotics and Automation. pp. 6035–6042. IEEE (2023) [4](#)
44. Xu, R., Tu, Z., Xiang, H., Shao, W., Zhou, B., Ma, J.: Cobevt: Cooperative bird’s eye view semantic segmentation with sparse transformers. In: Conference on Robot Learning (2022) [4](#)

45. Xu, R., Xia, X., Li, J., Li, H., Zhang, S., Tu, Z., Meng, Z., Xiang, H., Dong, X., Song, R., et al.: V2v4real: A real-world large-scale dataset for vehicle-to-vehicle cooperative perception. In: IEEE/CVF Conference on Computer Vision and Pattern Recognition. pp. 13712–13722 (2023) [1](#)
46. Xu, R., Xiang, H., Han, X., Xia, X., Meng, Z., Chen, C.J., Correa-Jullian, C., Ma, J.: The opencda open-source ecosystem for cooperative driving automation research. IEEE Transactions on Intelligent Vehicles **8**(4), 2698–2711 (2023). <https://doi.org/10.1109/TIV.2023.3244948> [10](#)
47. Xu, R., Xiang, H., Tu, Z., Xia, X., Yang, M.H., Ma, J.: V2x-vit: Vehicle-to-everything cooperative perception with vision transformer. In: European Conference on Computer Vision. pp. 107–124. Springer (2022) [2](#), [4](#), [5](#), [6](#), [10](#)
48. Xu, R., Xiang, H., Xia, X., Han, X., Li, J., Ma, J.: Opv2v: An open benchmark dataset and fusion pipeline for perception with vehicle-to-vehicle communication. In: International Conference on Robotics and Automation. pp. 2583–2589. IEEE (2022) [2](#), [4](#), [5](#), [6](#), [10](#), [12](#)
49. Yang, K., Yang, D., Zhang, J., Li, M., Liu, Y., Liu, J., Wang, H., Sun, P., Song, L.: Spatio-temporal domain awareness for multi-agent collaborative perception. IEEE/CVF International Conference on Computer Vision (2023) [4](#)
50. Yu, H., Luo, Y., Shu, M., Huo, Y., Yang, Z., Shi, Y., Guo, Z., Li, H., Hu, X., Yuan, J., et al.: Dair-v2x: A large-scale dataset for vehicle-infrastructure cooperative 3d object detection. In: IEEE Conference on Computer Vision and Pattern Recognition. pp. 21361–21370 (2022) [4](#)
51. Zeadally, S., Guerrero, J., Contreras, J.: A tutorial survey on vehicle-to-vehicle communications. Telecommunication Systems **73**(3), 469–489 (2020) [4](#)
52. Zhang, H., Zhang, Y.F., Liu, W., Weller, A., Schölkopf, B., Xing, E.P.: Towards principled disentanglement for domain generalization. In: IEEE/CVF Conference on Computer Vision and Pattern Recognition. pp. 8024–8034 (2022) [5](#)
53. Zhou, K., Liu, Z., Qiao, Y., Xiang, T., Loy, C.C.: Domain generalization: A survey. IEEE Transactions on Pattern Analysis and Machine Intelligence (2022) [5](#)
54. Zhou, K., Yang, Y., Hospedales, T., Xiang, T.: Deep domain-adversarial image generation for domain generalisation. In: AAAI Conference on Artificial Intelligence. vol. 34, pp. 13025–13032 (2020) [5](#)
55. Zhou, K., Yang, Y., Hospedales, T., Xiang, T.: Learning to generate novel domains for domain generalization. In: European Conference on Computer Vision. pp. 561–578. Springer (2020) [5](#)